Dup
A018 753

TECHNICAL
LIBRARY

TECHNICAL REPORT 4874

ELECTRIC FIELD EFFECTS IN ALPHA LEAD AZIDE SINGLE CRYSTALS USING AU-AU CONTACTS

U.S. ARMY PICATINNY ARSENAL

D. S. DOWNS
T. GORA
M. BLAIS
W. L. GARRETT

19971014 123

NOVEMBER 1975

DTIC QUALITY INSPECTED 8

PICATINNY ARSENAL

DOVER, NEW JERSEY

The findings in this report are not to be construed as an official Department of the Army Position.

DISPOSITION

REPORT DOCUMENTATION PAGE		READ INSTRUCTIONS BEFORE COMPLETING FORM
1. REPORT NUMBER Technical Report 4874	2. GOVT ACCESSION NO.	3. RECIPIENT'S CATALOG NUMBER
4. TITLE (and Subtitle) ELECTRIC FIELD EFFECTS IN ALPHS LEAD AZIDE SINGLE CRYSTALS USING AU-AU CONTACTS		5. TYPE OF REPORT & PERIOD COVERED
		6. PERFORMING ORG. REPORT NUMBER
7. AUTHOR(s) D. S. Downs, T. Gora, M. Blais, and W. L. Garrett		8. CONTRACT OR GRANT NUMBER(s)
9. PERFORMING ORGANIZATION NAME AND ADDRESS Explosives Division Picatinny Arsenal Dover, NJ 07801		10. PROGRAM ELEMENT, PROJECT, TASK AREA & WORK UNIT NUMBERS
11. CONTROLLING OFFICE NAME AND ADDRESS		12. REPORT DATE November 1975
		13. NUMBER OF PAGES 38
14. MONITORING AGENCY NAME & ADDRESS(if different from Controlling Office)		15. SECURITY CLASS. (of this report) Unclassified
		15a. DECLASSIFICATION/DOWNGRADING SCHEDULE

16. DISTRIBUTION STATEMENT (of this Report)

Approved for public release; distribution unlimited.

17. DISTRIBUTION STATEMENT (of the abstract entered in Block 20, if different from Report)

18. SUPPLEMENTARY NOTES

19. KEY WORDS (Continue on reverse side if necessary and identify by block number)

Initiation	Electrical contacts
Lead azide	Thermal initiation
Ignition	Current injection
Electric fields	Breakdown field

20. ABSTRACT (Continue on reverse side if necessary and identify by block number)

The response of single crystals of α-lead azide to moderately high electric fields has been investigated using Au contacts in a configuration that minimizes surface currents. Initiation is observed to occur at a threshold electric field of approximately 35,000 V/cm. Initiation cannot be attributed to bulk joule heating. The possibility that a space-charge-limited single carrier injection regime occurs at fields below the threshold field is assessed and tentatively rejected. Other possible mechanisms for

20. Continued

the current voltage characteristics and for the observed field initiation
are briefly discussed.

TABLE OF CONTENTS

Figures

INTRODUCTION

A number of azide compounds including lead azide are known to detonate when subjected to voltages or fields of sufficient strength (Ref 1, 4). A considerable reduction in the values of voltage or field necessary for initiation upon application of low-intensity irradiation of appropriate wavelength was recently reported by us (Ref 5). The mechanisms involved in these phenomena are not understood in detail although they appear to involve electronic processes (Ref 5). A complete experimental characterization of these phenomena is essential to their detailed understanding. We have completed the first step in such a characterization by studying the response of unilluminated lead azide single crystals to electric fields using evaporated Au-contacts in a particular geometric configuration.

The results are of interest in another important context. The problem of the sensitivity of lead azide to static electricity and to electric discharge has received considerable attention because of practical considerations relating to safety of storage and handling (Ref 6, 8). Studies in this area have typically been made on lead azide powders. It would appear, however, that a fundamental understanding of this sensitivity must be based upon a knowledge of the effects of electric fields on lead azide in its pure crystalline form.

The scope of our study was limited somewhat by the fact that our experiments involve the destruction of samples, and lead azide crystals suitable for our purposes are not routinely available in quantity. Hence, we concentrated on two goals. The first was to determine whether or not reproducible threshold values of either voltage or field are responsible for initiation. The second was to study the current-voltage characteristics of voltages below and near the initiation condition. Deviations from linearity can reveal electronic effects such as charge injection which may be involved in causing the initiation of lead azide.

EXPERIMENTAL

Single crystals of α-lead azide were grown by slow cooling from an ammonium acetate solution, following the method developed by Garrett (Ref 9) in this laboratory.

1

Several crystals were wafered using a string saw with a weak solution of ceric-ammonium-nitrate wetting the string. These wafers were then polished on both sides using very fine aluminum oxide abrasives. It should be noted that the wafers were not all sliced perpendicular to the same crystallographic direction.

Vacuum-evaporated gold electrodes were applied to both sides of the wafers. These gold electrodes were then contacted by gold wires using dots of silver paint. Figure 1 shows a typical wafer with the gold electrode applied. Sample thicknesses varied from .019 to .076 cm in this series of experiments. The electrode area was kept constant at .04 cm^2. The crystal mounting is shown schematically in Figure 2.

A sandwich type electrode configuration was chosen because surface currents can then be essentially eliminated; the entire sample-electrode system was potted in RTV, a polymeric electrode potting compound which further aids in prohibiting the flow of current by any path other than through the bulk of the sample. By keeping the evaporated electrode diameter large compared to the sample thickness, the results can be analyzed on the basis of one-dimensional planar current flow.

The circuitry and experimental procedures were kept as simple as possible. The circuitry, shown in Figure 3, consists of a regulated D.C. power supply, picoammeter, and strip chart recorder. RG-59/U shielded cable was used to connect the components. A 2-ma fuse was placed in series with the sample to protect the input resistor of the picoammeter from the large transient current which occurs at detonation.

The sample chamber, shown in Figure 4, was evacuated by a fore-pump with an in-line liquid nitrogen trap. With samples of the size used in these experiments, the chamber is not damaged by the explosion. Our experience has been that performing the experiments under this type of vacuum is sufficient to eliminate any dependence of the results on atmospheric humidity conditions.

A serious procedural difficulty arose because of the possibility that lead azide crystals subject to high electric fields can experience localized decomposition or other damage. This would act as a memory of prior treatment and might be expected to influence both conductivity and critical field for detonation. One way around this difficulty would involve using a fresh crystal of particular thickness for each separate voltage measurement. This procedure would, however, have demanded far more samples of accurately controlled thickness than we could prepare.

To minimize possible deviations caused by memory effects, we decided to subject each sample to the same voltage history. Our procedure involved one-minute-on, one-minute-off application of voltage, increasing the voltage in 100V increments as illustrated in Figure 5. The procedure was continued until the sample detonated with current being monitored continuously. Because sample thickness was a variable, it should be noted that all samples were not subjected to the same field history.

The experiments were performed at room temperature ($\sim$300K), and the samples were not illuminated.

RESULTS

Figure 5 shows the typical current response to the applied voltage steps. There is an undershoot when the voltage is turned off which is not shown. Seven samples of varying thickness were investigated in this manner. The magnitude of the current I just prior to detonation and the average electric field strength at detonation V_{det}/L are shown in Table 1. It should be noted that the detonation does not necessarily occur immediately upon application of the voltage. The time lag was observed to vary. We have also plotted the logarithm of the current observed after one minute, versus the logarithm of the applied voltage. These results appear in Figures 6-12.

DISCUSSION

Table 1 shows that the voltages at which detonation occurred (V_{det}) ranged from 800 to 2700V. Thus it would hardly make sense to speak of a threshold voltage. One would expect a voltage threshold if the voltage drop occurred primarily at the electrodes. If the voltage drop across the sample is relatively uniform, the bulk of the sample experiences an electric field near the average field, defined as V_{det} divided by sample thickness L. The average fields at which detonation occurred are rather more closely grouped, these ranging from 30,250 to 42,000 V/cm. It thus appears that there is a threshold average field at which detonation occurs in this field range. The scatter in values would then be accounted for by sample differences beyond our control, including perhaps deviations in the uniformity of voltage drop or differences due to crystal orientation.

3

Note that the threshold field values for the four thinnest samples
(.019 - .025 cm) are all higher than those for the thicker samples
(.043 - .076 cm). This would be expected if damage resulting from
exposure to fields tends to lower the field threshold, since the
thicker samples experienced longer cumulative exposure times to
fields.

We now turn to a discussion of the current-voltage characteris-
tics. Since no attempt was made to eliminate capacitance from the
external circuit, the initial capacitive spike which occurs imme-
diately upon application of the voltage does not accurately represent
current through the sample. (The peak current was linear with volt-
age over the entire voltage range for all samples.) The current at
the end of one minute, although not strictly steady state, was taken
to represent the response of the current through the crystal to
applied voltage.

The log I-log V plots of the seven samples are not all similar
(Figures 6-12). Portions of some of them show regions where current
depends rather clearly on V, V^2, and/or V^3 and some contain discon-
tinuities. The variance in these I-V characteristics is rather puzz-
ling. Perhaps the most significant feature is that superlinear
regions occur in all but one case. One possible explanation is that
these regions are caused by space-charge-limited (SCL) current flow
arising from single carrier current injection.

Current injection phenomena in solids have been reviewed by
Lampert and Mark (Ref 10). We shall outline those features that may
be relevant to this work. The first criterion for injection to occur
is the existence of an injecting contact, one that by definition
supplies a reservior of carriers freely available to enter the insula-
tor as needed. Lead azide has a band gap of approximately 3.5eV
(Ref 11, 12) and the electron affinity has been found to be about
1.2eV (Ref 13). With gold contacts on lead azide single crystals,
it is expected that near the azide-electrode interface, the lead
azide valence band may be bent to the Fermi level, forming an inject-
ing contact for holes. This expected energy band scheme is schema-
tically depicted in Figure 13a. Because of its relatively large
work function, gold would not be expected to form an injecting con-
tact for electrons. It has been shown (Ref 10) that in the presence
of thermally generated free carriers and no carrier traps, SCL cur-
rent flow is characterized by an ohmic I-V relation at low voltages,
and a quadratic one at higher voltages. The presence of traps can
lead to discontinuities in the IV characteristics.

4

The problem with the SCL current interpretation is that recent internal photoemission studies (Ref 14) indicate that gold forms a blocking (non-injecting) contact to PbN_6 under the preparation conditions used here. This is depicted in Figure 13b. Thus the super-linear I-V relations cannot be explained by SCL current flow. Either high-field effects (in which, e.g., the mobility is a function of field), or field lowering of the (blocking) barrier might then be responsible (Ref 15).

It is not possible at this time to identify the phenomena which lead to initiation. Some comments are, however, possible. Initiation is not caused by bulk joule heating. The power input prior to initiation, IV, is typically 10^{-5} watts. Total energy input up to initiation is of the order of 10^{-3} calories distributed over a volume of $10^{-2} cm^3$ (.2cm x .04cm^2). For lead azide, the density (Ref 16) is 4.7gm/cm^3 and the specific heat (Ref 1) 0.10cal/gm-K. Even when all energy loss processes are neglected, this leads to temperature increases of only about 0.2K, which would not be expected to cause initiation.

Temperature rises could be much higher if the current density were concentrated near one electrode, for example, or in a small-diameter filament stretching from one electrode to the other. The first possibility can be rejected partly because the relatively constant threshold electric field value suggests that the voltage drops rather uniformly across the bulk of the crystal. Further, the rapid rate of thermal diffusion, in this essentially one-dimensional geometry, makes it impossible to achieve thermal initiation by joule heating no matter how thin a laminar region the voltage drop occurs over on our time scale. Indeed, a temperature rise of only 0.1K is expected (see Appendix). For the case of filamentary conduction, thermal initiation by joule heating is also impossible, with a temperature rise of about 1K (see Appendix). Finally, for the case of all the energy input being confined to a small point-like region in the crystal (a rather unusual physical situation), thermal initiation is indeed possible on a time scale of approximately 10^{-8} secs (see Appendix). Such short time scales for initiation run counter to our observations and are not consistent with our observed thresholds.

Other possible phenomena that could lead to initiation would appear to be essentially non-thermal. Dielectric breakdown at these low current densities, for example, involves a manyfold multiplication of current carriers (electrons and/or holes). Such multiplication requires quanta of energy in the electron-volt range, which are in extremely short supply at normal temperatures. Any temperature rises associated with exothermic reaction would themselves have been

5

induced by the presence of electron and/or hole densities in excess of the small density available in the absence of the electric field.

McLaren and Rogers (Ref 17) have reported that AgN_3 initiates under applied fields of ca 250 V/cm. Bowden and McLaren (Ref 2) suggest that this is caused by field emission from the cathode. In this model electrons enter the crystal with sufficient energy to produce decomposition (because of space-charge fields), followed by self-heating and explosion. While such a model may possibly apply to our results in PbN_6, two factors should be noted. Our currents are four orders of magnitude lower than those observed in AgN_3 even for much higher fields. And, as we have mentioned, the voltage drop in our experiments appears to be relatively uniform across our crystals at least up to or near initiation.

Whereas the present report finds that average fields of 3.5 x 10^4 V/cm lead to initiation for PbN_6 crystals using Au-Au contacts, PbN_6 crystals and pellets with capacitively coupled electrodes can withstand average fields of 1-2 x 10^5 V/cm without visible damage (Ref 18). The role of the contacts is thus seen to be important in field initiation, and a combined experimental and theoretical effort to examine that role will be reported elsewhere (Ref 18).

Table 1

Electric field effects on lead azide

Sample	Thickness L(cm)	Current at detonation (amp)	Voltage at detonation V_{DET}	Threshold field V_{DET}/L (volts/cm)
3-72-30	.019	1.2×10^{-9}	800	4.20×10^4
3-72-31	.024	6.9×10^{-8}	1000	4.17×10^4
3-72-32	.022	7.0×10^{-9}	800	3.60×10^4
3-72-33	.043	1.6×10^{-8}	1300	3.02×10^4
3-72-34	.025	1.4×10^{-8}	1000	4.00×10^4
3-72-35	.076	5.5×19^{-9}	2700	3.54×10^4
3-72-36	.073	1.1×10^{-8}	2400	3.26×10^4
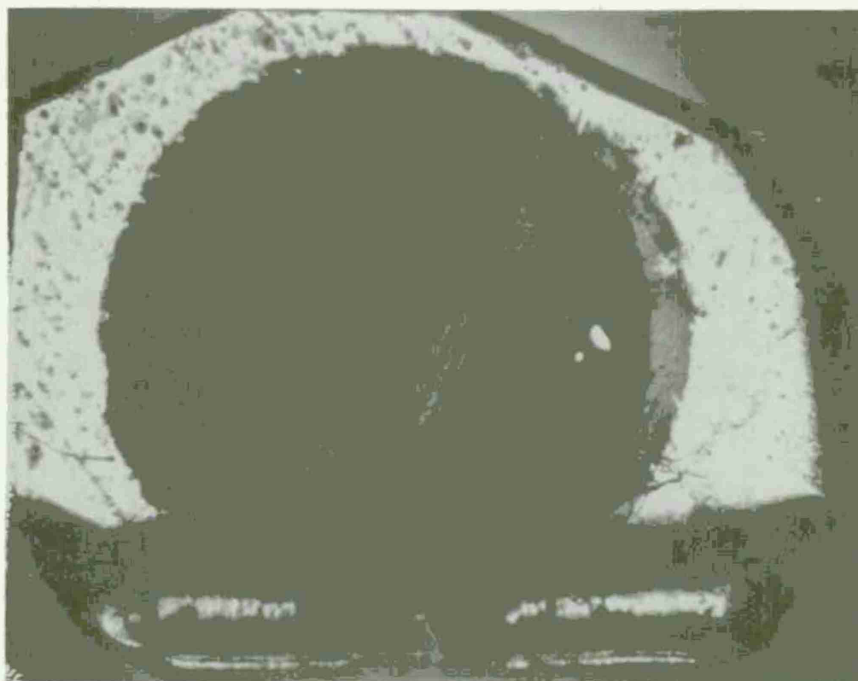
Fig 1   Single crystal of PbN$_6$ with evaporated gold
        electrode.   (Dimension $\sim$0.3 x 0.4 x .02 cm)

SCHEMATIC OF SAMPLE MOUNTING

CRYSTAL

TEFLON   GOLD   LEADS

SILVER
PAINT

RTV

GOLD
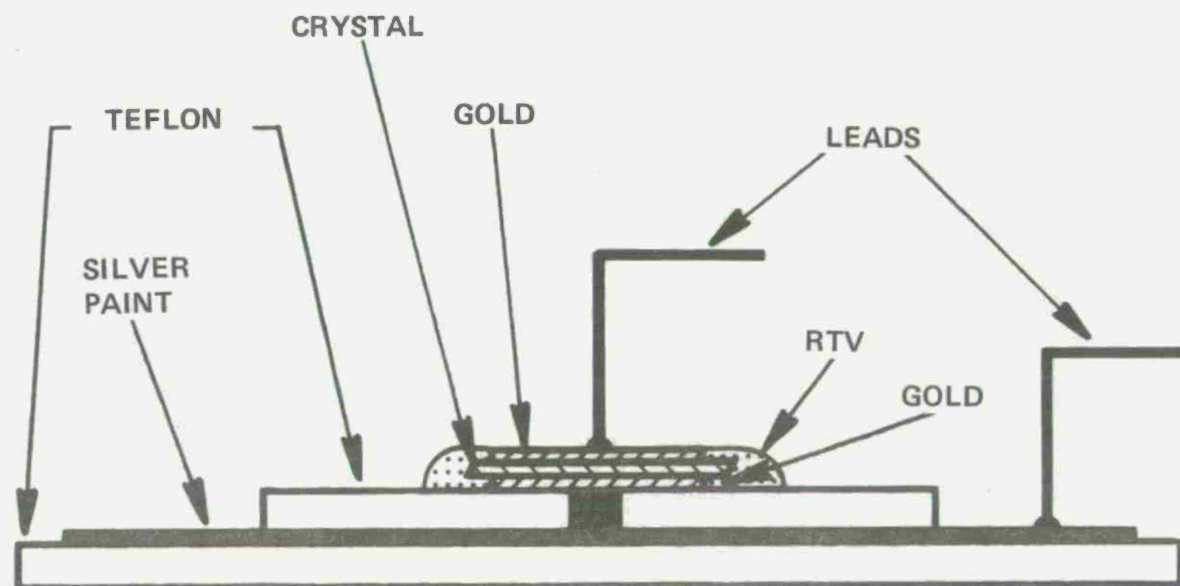
Fig 2   Crystal mounted for measurements

SAMPLE   PICOAMMETER

RECORDER
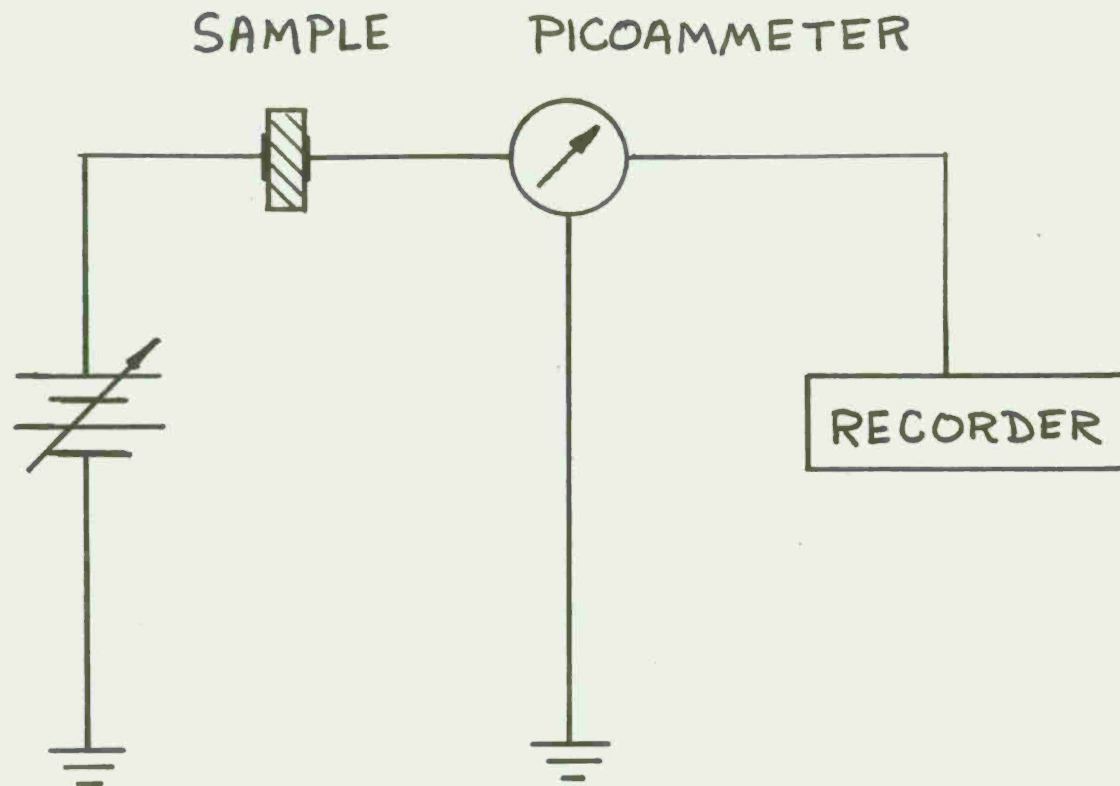
Fig 3   Schematic of measuring circuit
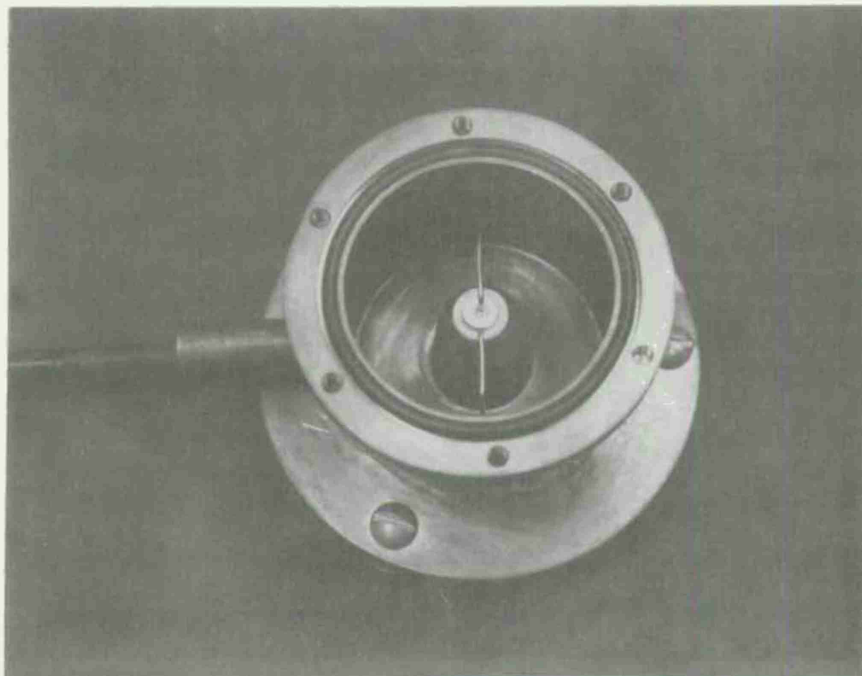
Fig 4   Sample chamber

11
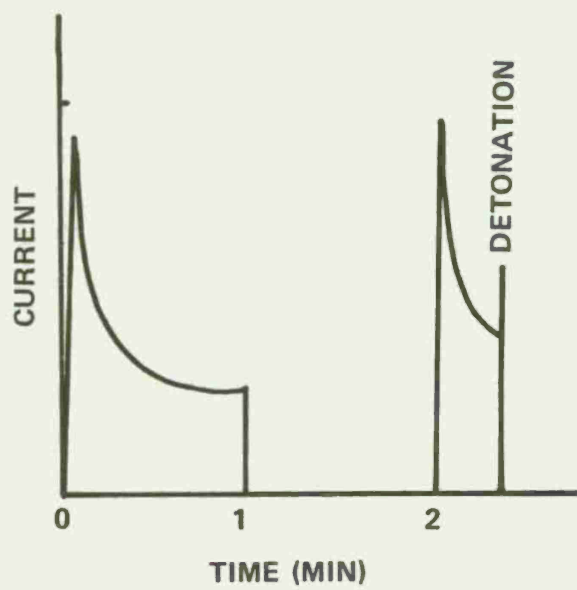
Fig 5   Typical current response to step
increases in voltages

12
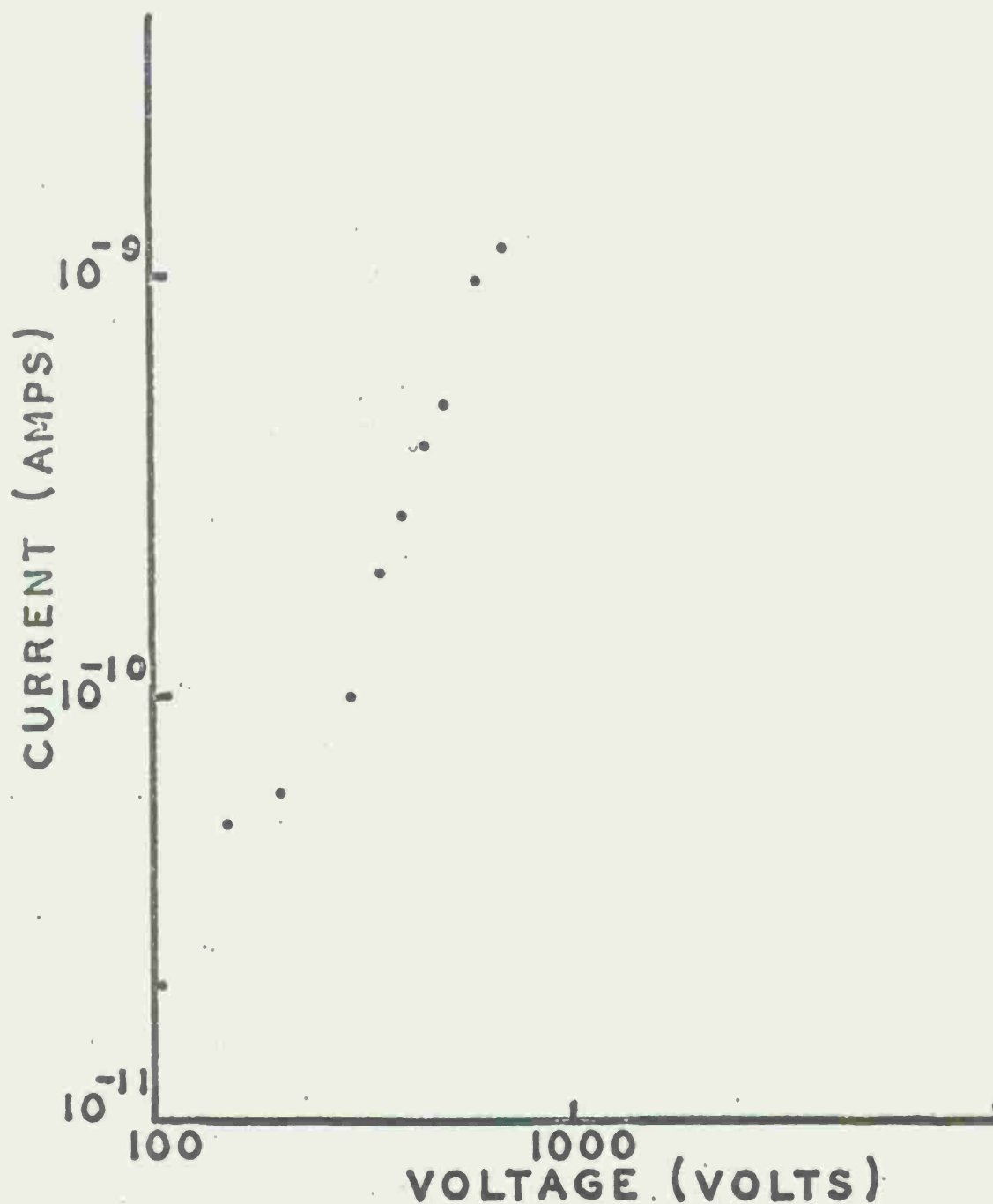
Fig 6   Current - Voltage characteristic
        (.019 cm thick)

13
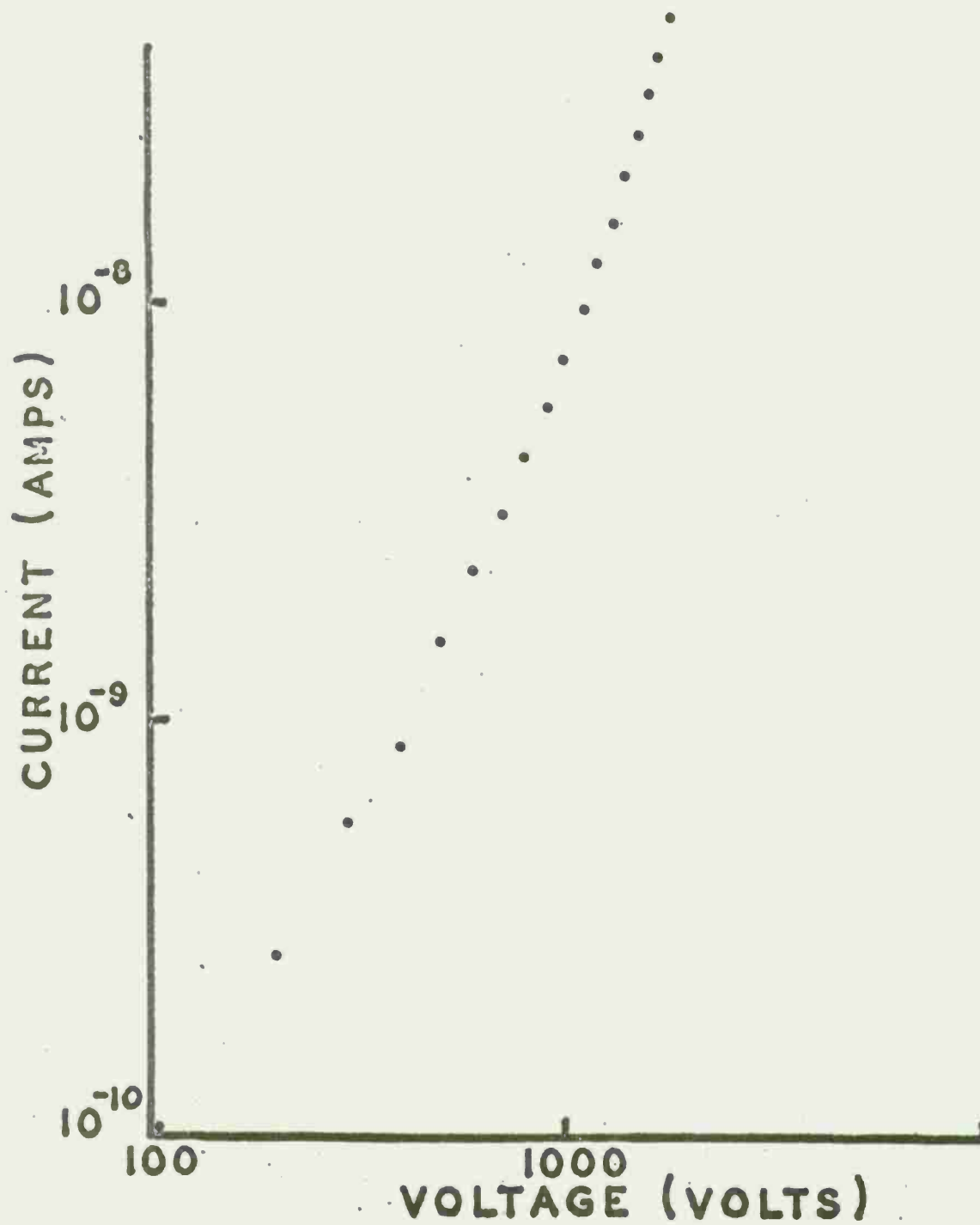
Fig 7   Current - Voltage characteristic
         (.024 cm thick)

14
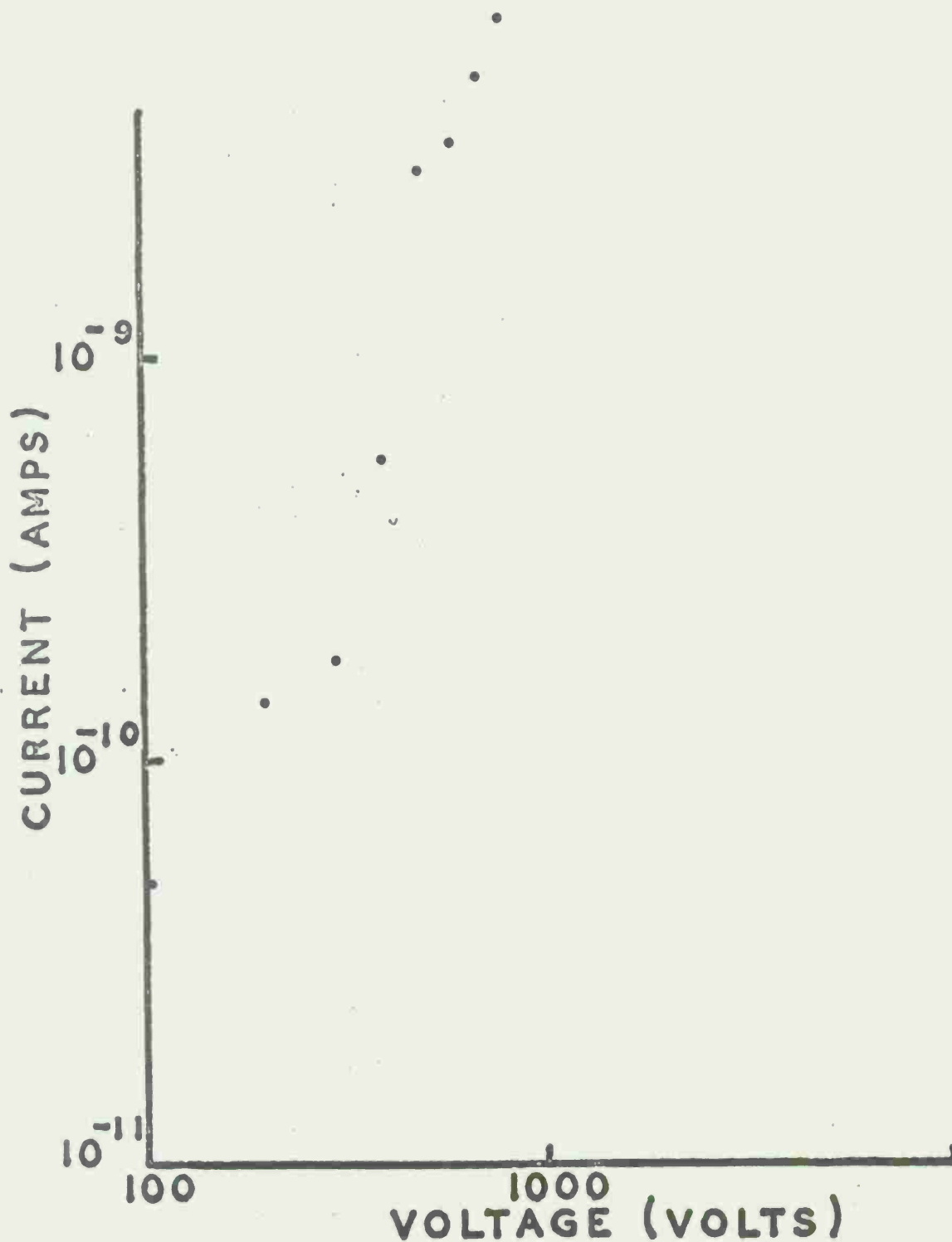
Fig 8   Current - Voltage characteristic
          (.022 cm thick)

15
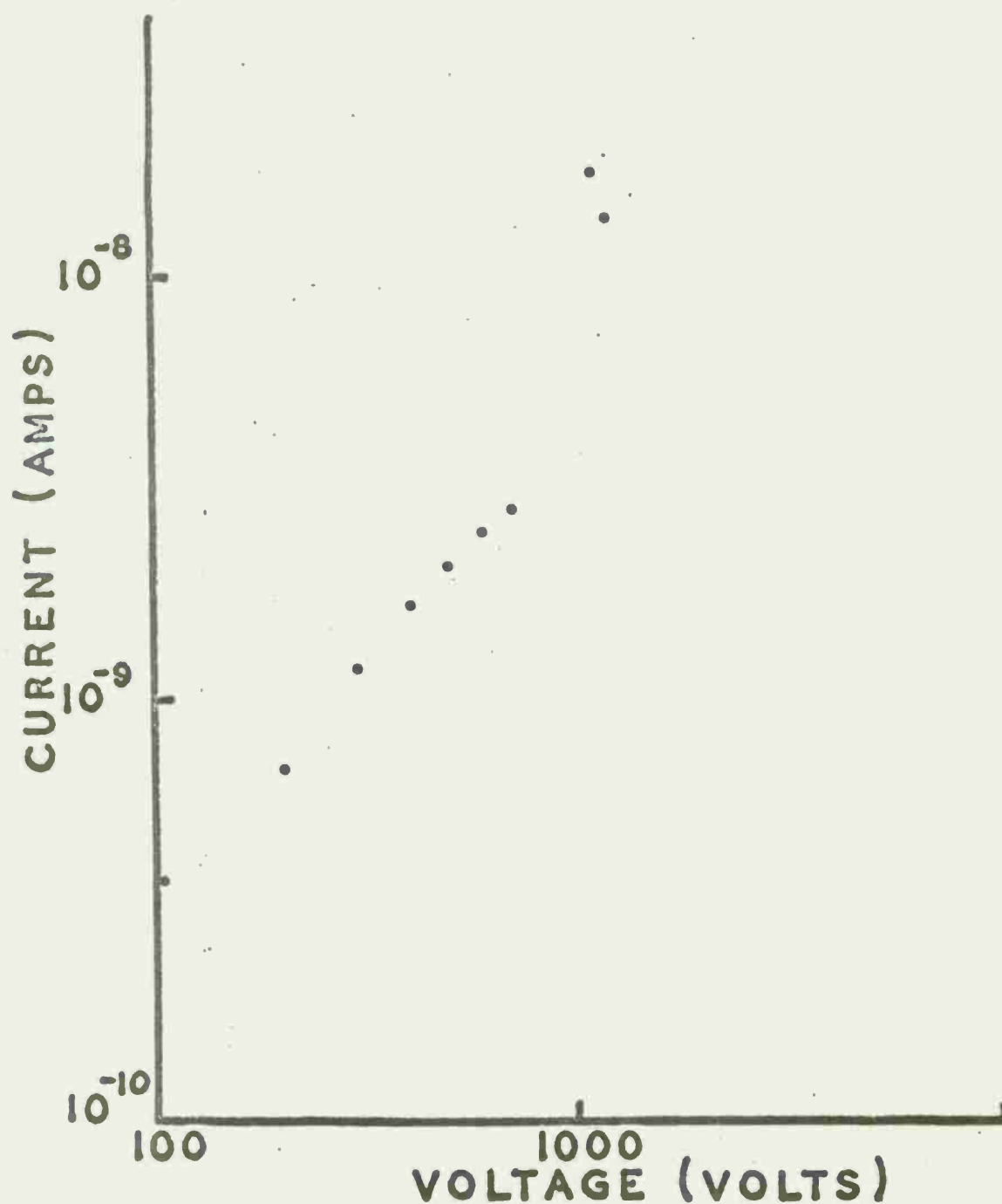
Fig 9   Current - Voltage characteristic
         (.043 cm thick)

Fig 10   Current - Voltage characteristic
          (.025 cm thick)

17

Fig 11   Current - Voltage characteristic
(.076 cm thick)

18
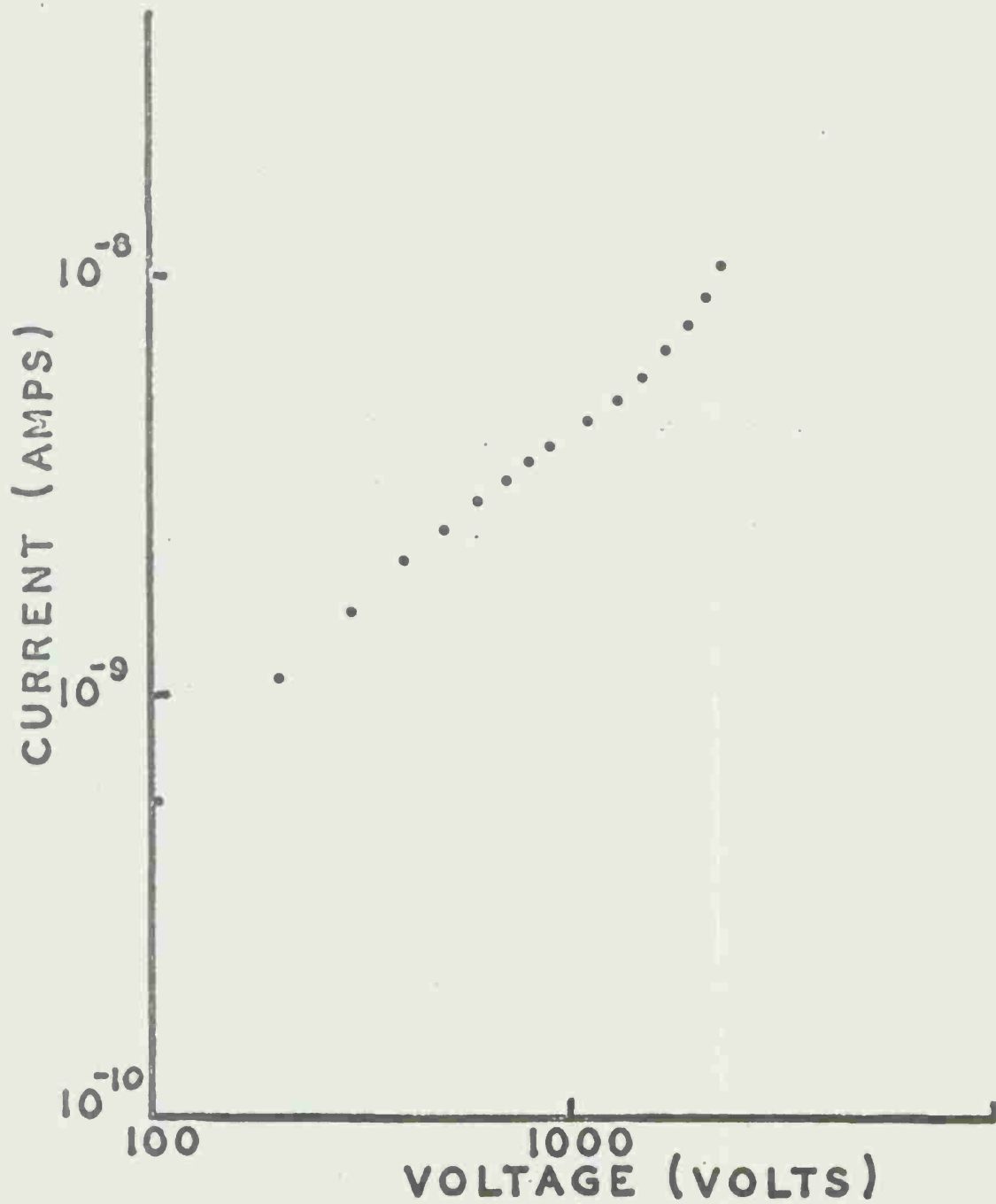
Fig 12   Current - Voltage characteristic
         (.073 cm thick)

GOLD   PbN$_6$

– – – – E_F

(a)

GOLD   PbN$_6$

– – – – E_F

Φ_B

(b)

Fig 13   Band picture of (a) an ohmic contact for holes
and (b) a blocking contact for holes; E_F is the
Fermi level, and Φ_B the barrier height

APPENDIX

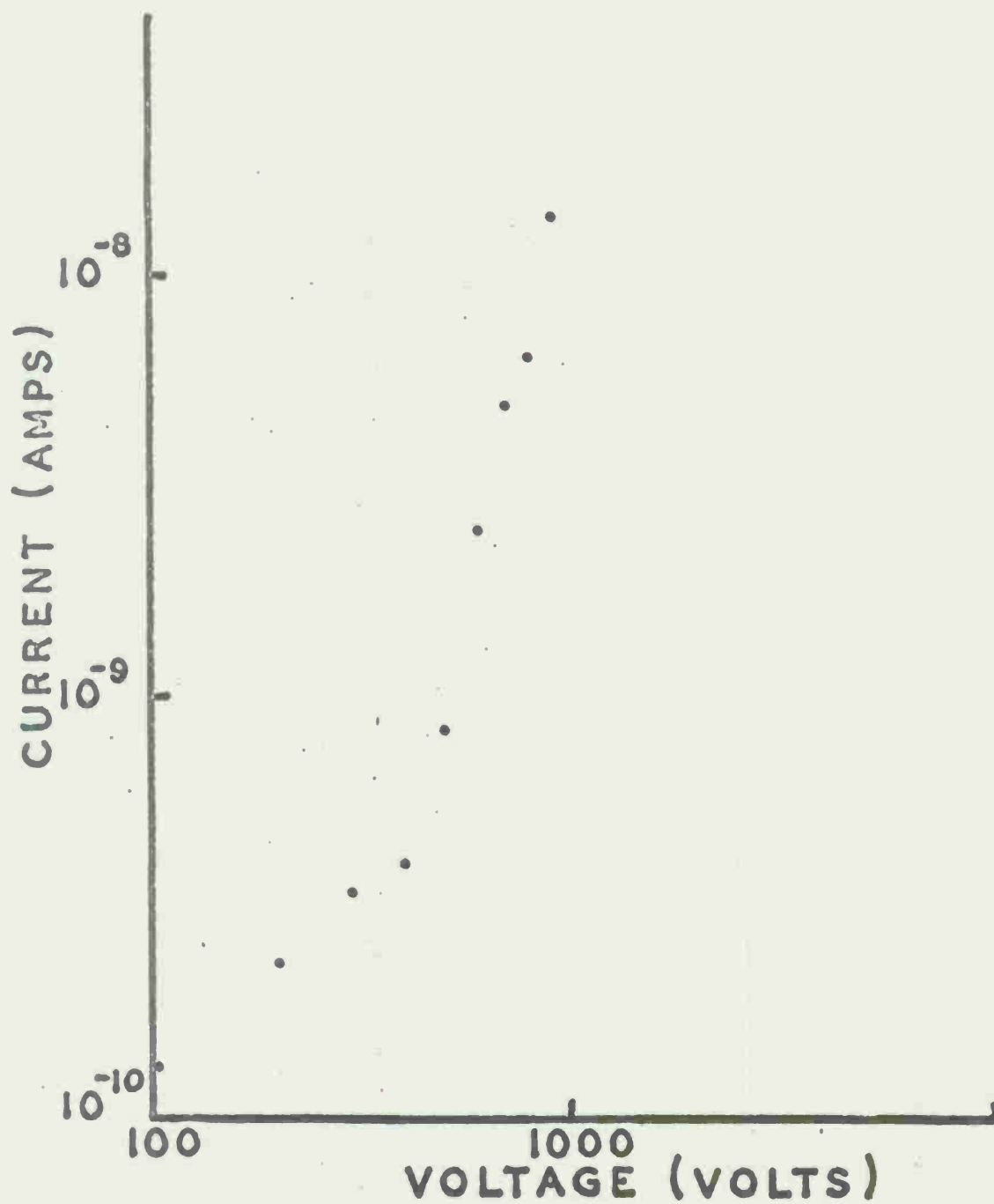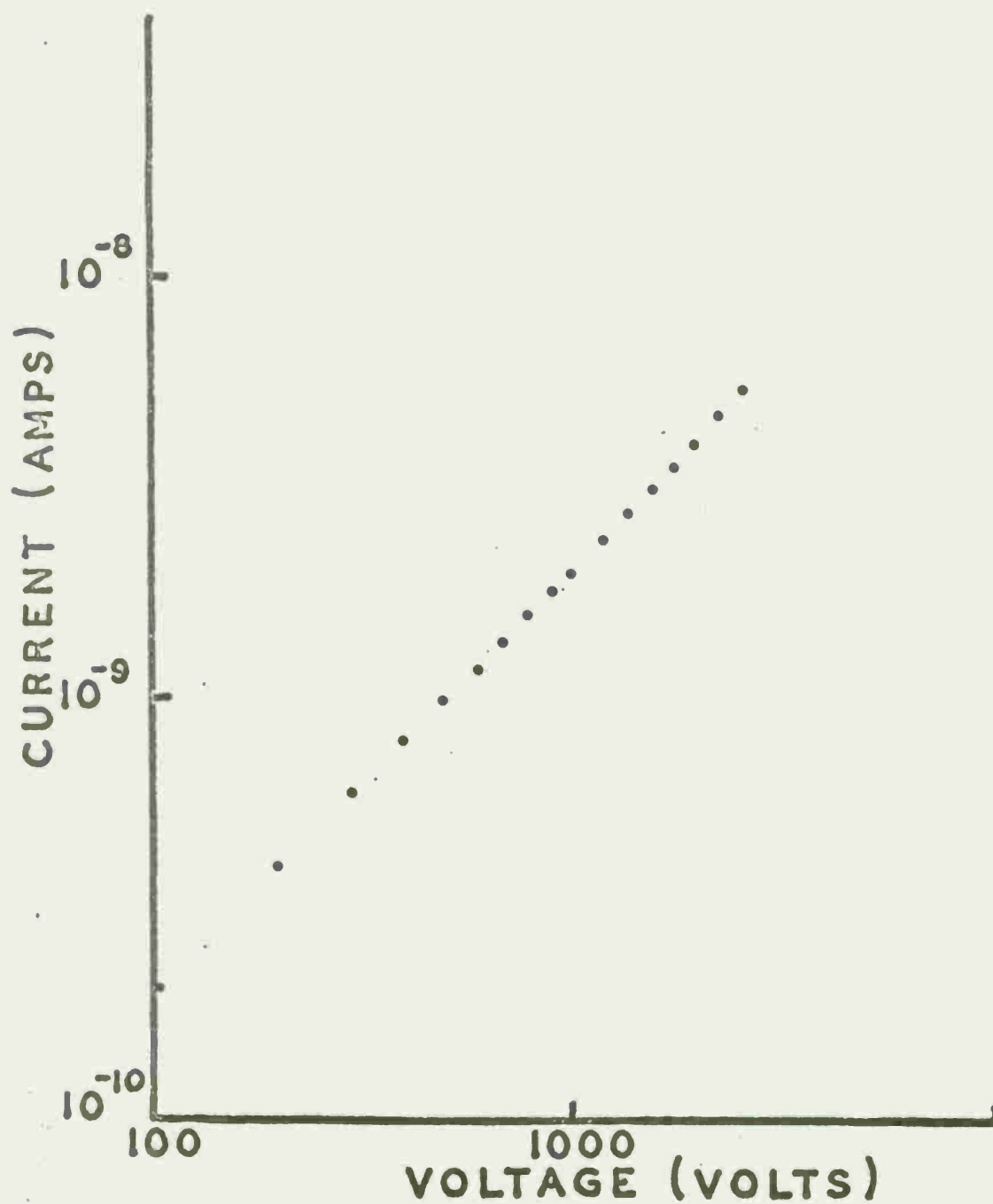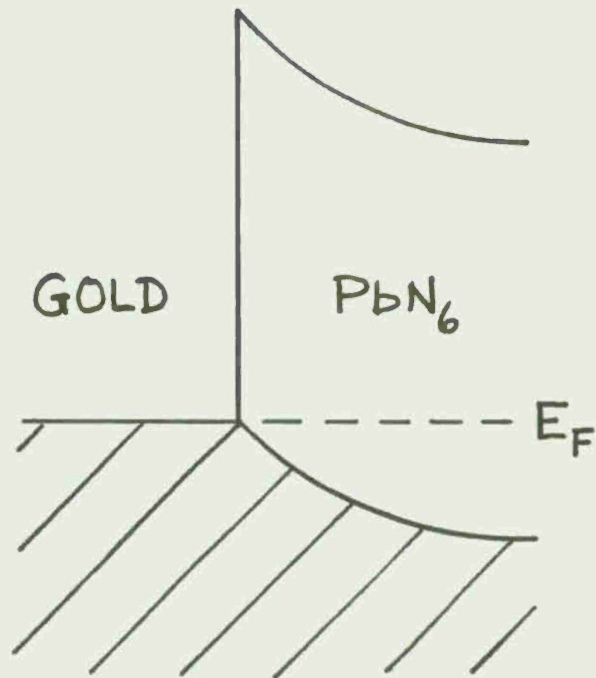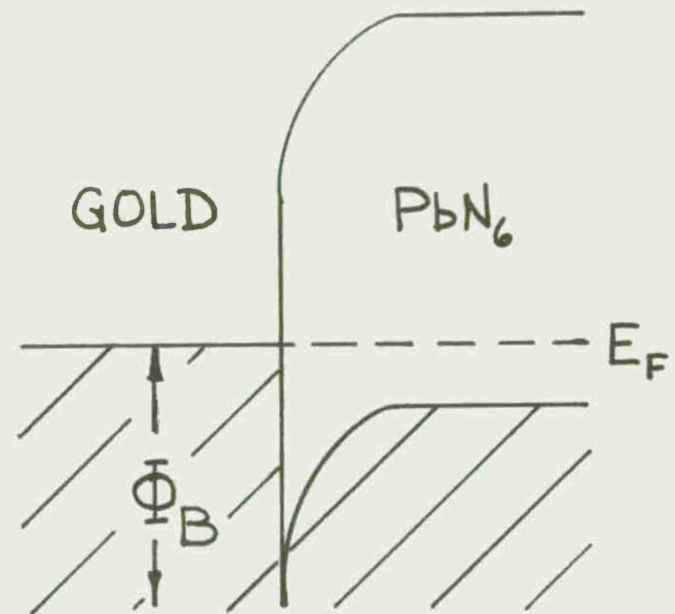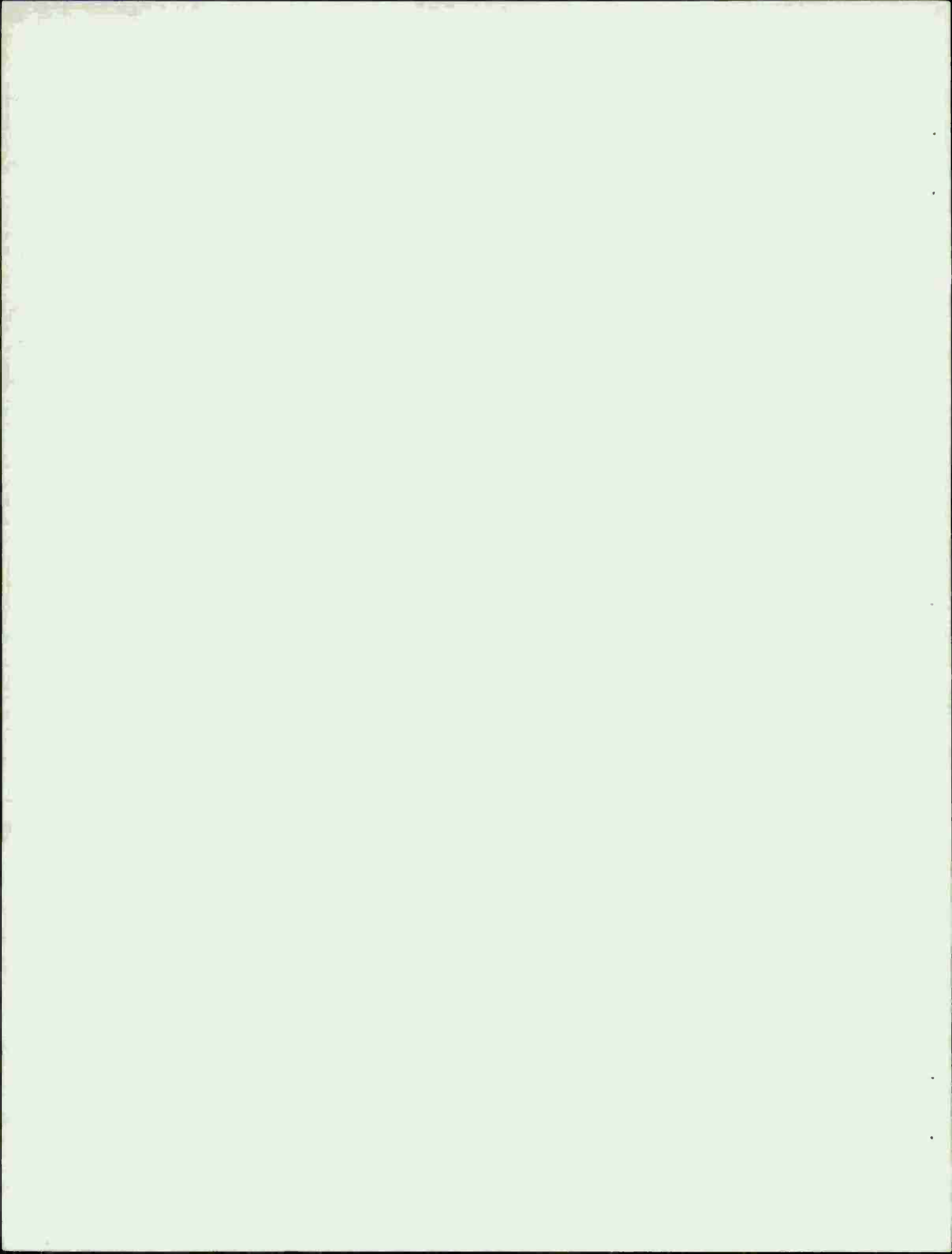It was shown in the text that for our experiments, bulk joule heating of the entire crystal would lead to insignificant temperature rises. We examine here the consequences of more localized joule heating, as would occur when either the current or voltage drop is not uniformly distributed. Some conclusions are possible on the basis of rather simple models. For purposes of comparison, the explosion temperature (minimum temperature for ignition in 5 seconds) for lead azide is 315°C (Ref 1).

Our basic assumptions are: Energy input occurs primarily through joule heat, i.e., self-heating by exothermic chemical decomposition is not important at temperatures well below the explosion temperature. Energy delocalization is effected primarily by thermal conduction. This is certainly valid for a lower limit (upper limit on temperature rise), as other modes of energy transport (such as radiative processes) can only increase the rate of energy delocalization. The material properties of lead azide needed are the density ρ and the specific heat c (values appear in the text), and the thermal conductivity k. A value of 4.0×10^{-4} cal/°C cm-sec is assumed for k (see Ref 1, although there is ambiguity in the units quoted). All are assumed to be independent of temperature. The value for k is for a pressed pellet. One would expect a higher value for single crystals, so that again the assumptions are consistent with a lower limit for rate of energy delocalization. The quantities ρ and c will appear in the thermal diffusivity κ, defined as $\kappa = \dfrac{k}{\rho c}$.

One-Dimensional Geometry

We first examine the temperature rise with time for the case where the voltage drop occurs across an infinitely thin plane parallel to the electrodes. This can happen either within the lead azide crystal or near one of the electrodes. The physical system is then reasonably approximated, at least for an upper limit of temperature rise τ, by the adjoining semi-infinite regions depicted in Figure A-1 with thermal diffusivity κ and thermal conductivity k defined in each region. For time t>0, heat is supplied at the constant rate F_0 per unit time per unit area in the plane x=0.

The thermal flux f is then defined as

$$f = -k \frac{\partial \tau}{\partial t} \tag{A-1}$$

23

and satisfies the differential equation

$$\kappa_{\frac{1}{2}} \frac{\partial^2 f}{\partial x^2} = \frac{\partial f}{\partial t} \, ,$$

where κ_1 is used for x<0 and κ_2 for x>0.

The solution for τ, by well-known methods (Ref 19), is

$$\tau = \frac{2F_{\frac{1}{2}} (\kappa_{\frac{1}{2}} t)^{1/2}}{k_{\frac{1}{2}}} \text{ ierfc } \frac{|x|}{2(\kappa_{\frac{1}{2}} t)^{1/2}}. \qquad (A-2)$$

The upper subscript is used for x<0 and the lower for x>0. The function ierfc (λ) is defined as

$$\text{ierfc } (\lambda) \equiv \frac{1}{\sqrt{\pi}} e^{-\lambda^2} - \lambda \text{ erfc } (\lambda), \qquad (A-3)$$

where

$$\text{erfc } (\lambda) \equiv \frac{2}{\sqrt{\pi}} \int_\lambda^\infty e^{-y^2} \, dy. \qquad (A-4)$$

The latter function, commonly occurring in heat conduction problems, is tabulated in a number of placed (Ref 19). The quantities F_1 and F_2 are determined by the conditions

$$\frac{F_1 \kappa_1^{1/2}}{k_1} = \frac{F_2 \kappa_2^{1/2}}{k_2} \text{ and } F_1 + F_2 = F_o \qquad (A-5)$$

The highest temperature at any given time occurs at x=o, where the temperature τ_o is

$$\tau_o = \frac{1.128 \, F_2 \, (\kappa_2 t)^{1/2}}{k_2} \qquad (A-6)$$

24

If the sudden voltage drop occurs well within the crystal, clearly $F_1 = F_2 = F_o/2$. Under the conditions of our experiment, $F_o \approx 6 \times 10^{-5}$cal/sec-cm^2 when the voltage is on. Plugging in values for the thermal properties k and κ, one finds (for t in seconds) $\tau_o \approx 2 \times 10^{-3}\ t^{1/2}$K. Thus for $t = 10^3$ secs, the maximum temperature rise resulting from joule heating for this case of rapid voltage drop is less than 0.1K. Should the sudden voltage drop occur near a gold contact, the corresponding temperature rise calculated using Equations (A-5) and (A-6) is two orders of magnitude lower because of the high thermal conductivity of gold. We conclude that even for abrupt voltage drops, our experimental power input is insufficient to cause thermal initiation of lead azide by simple joule heating temperature rises.

Two-Dimensional Geometry

We next examine the case of all the current flowing in a small filament joining, and perpendicular to, the electrodes. A reasonable idealization of this case is an infinitely thin constant line source of heat which begins emitting at t=0, embedded in an infinite lead azide crystal.

Radial distance from the line source is denoted by r. For this case, we search first for a solution to the heat conduction differential equation

$$\nabla^2 \tau = \frac{1}{\kappa} \frac{\partial \tau}{\partial t}, \tag{A-7}$$

subject to release at t=0 of an instantaneous uniform heat pulse of magnitude Q ρc (ρ is density, and c specific heat) per unit length of the line. The solution for all times t>0 can be shown to be

$$\tau = \frac{Q}{4\pi\kappa t}\ e^{-r^2/4\kappa t} \tag{A-8}$$

As $t \to 0$, τ also goes to zero for all r except r=0. There it becomes infinite in such a way that its integral over all space is finite. Physically this occurs because a finite amount of energy was assumed supplied to an infinitesimally small volume, that of the ideal line. In practice, heat cannot be released from an ideal

line source. Indeed, temperature is defined only in a statistical sense, and it therefore has no physical meaning when applied to regions of sub-atomic dimensions, i.e., for $r < 10^{-8}$ cm.

If now heat is released by the source continuously at the constant rate $\rho c q$ per unit time per unit length, the temperature is determined by integrating Equation (A-8) over time, i.e.,

$$\tau = \frac{q}{4\pi\kappa} \int_{0}^{\tau} e^{-r^2/4\kappa t'} \frac{dt'}{t'} . \tag{A-9}$$

Integration yields the function

$$\tau = -\frac{q}{4\pi\kappa} \text{ Ei } \left(-\frac{r^2}{4\kappa t}\right), \tag{A-10}$$

where

$$-\text{Ei } (-x) = \int_{x}^{\infty} \frac{e^{-u}}{u} \, du.$$

For small values of x,

$$\text{Ei } (-x) = \gamma + \ln(x) - x + \frac{x^2}{4} + 0(x^3), \tag{A-11}$$

where $\gamma = 0.5772$. For our present purposes, it will be the case that Ei(-x) is sufficiently approximated by the single term $\ln(x)$.

Under the conditions of our experiment $\rho c q \approx 10^{-4}$ cal/sec-cm. For $r = 10^{-8}$ cm and $t = 10^3$ sec, one finds from Equation (A-10) that $\tau < 1K$. Temperature rises of the order 100K can be realized for $r \approx 10^{-1000}$ cm, but we have shown that the concept of temperature is not physically meaningful for these dimensions. We conclude that even for the case of all the current flowing in a narrow filament through the crystal, our experimental power input is insufficient to cause thermal initiation of lead azide by simple joule heating temperature rises.

26

Three-Dimensional Geometry

We finally consider the case of both filamentary conduction and an abrupt voltage drop, so that all the energy input is delivered in a small volume of the crystal. This situation can be approximated by a continuous point source in an infinite medium.

The solution to the heat conduction differential Equation (A-7) for an instantaneous heat point source of magnitude ρcP, located at $r=0$ and delivered at $t=0$, can be shown to be

$$\tau = \frac{P}{(4\pi\kappa t)^{3/2}} \; e^{\frac{-r^2}{4\kappa t}} \, , \qquad\qquad (A-12)$$

for times $t>0$. The solution for a continuous steady heat point source of magnitude p per unit time is then obtained by integrating Equation (A-12) over time, and is

$$\tau = \frac{p}{e\pi\kappa r} \; \text{erfc} \; \frac{r}{(4\kappa t)^{1/2}} . \qquad\qquad (A-13)$$

The function erfc (λ) has been defined in Equation (A-4).

For $t\to\infty$ or for sufficiently small r, this reduces to $\tau = \frac{p}{4\pi\kappa r}$. Under the conditions of our experiments $p \approx 2 \times 10^{-6}$ cal/sec. It follows that temperature rises in excess of 100K are realized within a radius of $r \approx 4 \times 10^{-6}$ cm. We conclude that initiation by simple joule heating temperature rises is possible if all the power input is confined to a small point-like region of the crystal. Under these conditions initiation should in fact occur on a time scale of approximately 10^{-8} sec. The fact that our experiments show initiation occurring after many seconds tends to discredit the applicability of this type of mechanism. Further, this kind of mechanism would predict initiation for far lower fields than those observed to be necessary.

$$X = 0$$
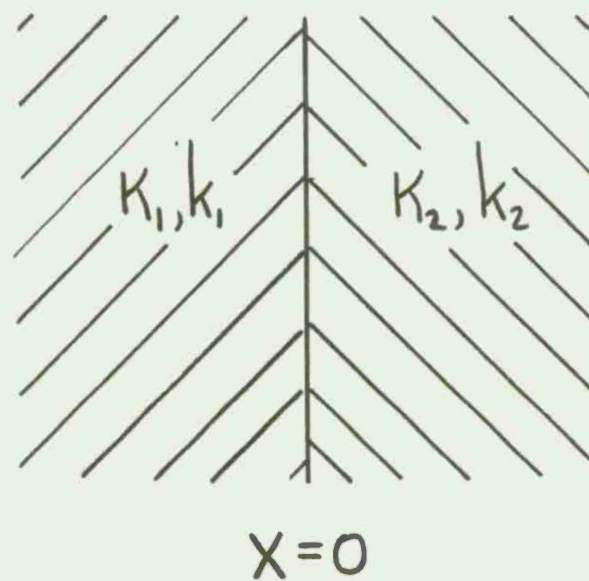
Fig A1   One-dimensional model for voltage drop across a thin plane at x=0. The adjoining media are characterized by thermal diffusivities and thermal conductivities κ_1, k_1 and κ_2, k_2.

28

REFERENCES

1. F. P. Bowden and A. D. Yoffee, Fast Reactions in Solids, Academic Press, New York, 1958.

2. F. P. Bowden and A. C. McLaren, Proc. Roy. Soc., A246, 197 (1958).

3. Yu. N. Sukhushin et al., Izv. Tomsk. Politekh. Inst., 251, 219 (1970).

4. Yu. A. Zakharov and Yu. N. Sukhushin, Izv. Tomsk. Politekh. Inst., 251, 213 (1970).

5. H. D. Fair, Jr. et al., Picatinny Arsenal Technical Report 4607, December 1973.

6. M. A. Mel'nikov et al., Russ. J. Phys. Chem., 44 (9), 1314 (1970).

7. C. R. Westgate et al., Picatinny Arsenal Technical Report 4319, April 1972.

8. R. M. H. Wyatt et al., Proc. Roy. Soc., A246, 189 (1958).

9. W. L. Garrett, Mat. Res. Bull., 7, 949 (1972).

10. M. A. Lampert and P. Mark, Current Injection in Solids, Academic Press, New York, 1970.

11. H. D. Fair, Jr. and A. C. Forsyth, J. Phys. Chem. Solids, 30, 2559 (1969).

12. T. Gora, J. Phys. Chem. Solids, 32, 529 (1971).

13. K. Hunter and F. Williams, private communication.

14. D. S. Downs, Picatinny Arsenal Technical Report, in preparation.

15. P. Mark, private communication.

16. Encyclopedia of Explosives and Related Items, (B. T. Federoff, ed.) Vol. 1, Compton Press, 1960.

17. A. C. McLaren and G. T. Rogers, Proc. Roy. Soc., A240, 484, (1957).

18. D. S. Downs, T. Gora and P. Mark (in preparation for the Journal of Solid State Chemistry).

19. H. S. Carlslaw and J. C. Jaeger, Conduction of Heat in Solids, Oxford University Press, London, 1959.

DISTRIBUTION LIST

Commander
Picatinny Arsenal
ATTN: Mr. H. W. Painter   1
        SARPA-TS-S   2-6
Dover, NJ   07801

Commander
U.S. Army Materiel Command
ATTN: AMCDL   7
        AMCRD   8
        AMCRD-T   9
        AMCRD-TC   10
5001 Eisenhower Avenue
Alexandria, VA   22333

Commander
U.S. Army Armaments Command
ATTN: AMSAR-RD-T   11
        AMSAR-SF   12
        AMSAR-RD, Dr. J. A. Brinkman   13
        AMSAR-ASF   14
Rock Island, IL   61201

Commander
U.S. Army Ballistic Research Laboratories
ATTN: Technical Library   15
        Dr. R. J. Eichelberger, Director   16
        Dr. I. May   17
        Dr. E. Freeman   18
Aberdeen Proving Ground, MD   21005

Commander
Army Research Office (Durham)
ATTN: Dr. D. R. Squire   19
        Dr. R. Ghirardelli   20
Box CM, Duke Station
Durham, NC   28806

Commander
U.S. Naval Weapons Center (Code 753)
ATTN: Technical Library   21
       Dr. R. Reed   22
       Mr. J. Pakulak   23
China Lake, CA 93555

Defense Documentation Center   24-35
Cameron Station
Alexandria, VA 22314

Commander
U.S. Naval Ordnance Laboratory
ATTN: Technical Library   36
       Mr. I. Kabik   37
       Mr. H. Leopold   38
White Oak, Silver Spring, MD 20910

Director
U.S. Naval Research Laboratory
ATTN: Code 2027   39
Washington, DC 20350

U.S. Naval Ordnance Station
ATTN: Library   40
Indian Head, MD 20640

Commander
Frankford Arsenal
Pittman-Dunn Laboratories
ATTN: Dr. J. Lannon   41
Bridge and Tacony Streets
Philadelphia, PA 19137

Explosives Research Laboratories
Bureau of Mines
ATTN: Dr. R. W. Watson   42
Pittsburg, PA 15230

Headquarters   43
Air Force Weapons Laboratory (WLX)
Kirtland Air Force Base, NM 87117

```
Commander
Armament Development & Test Center
Eglin AFB
ATTN:  Dr. L. Elkins                               44
Valpariso, FL   32542


Commander
Harry Diamond Laboratories
ATTN:  Technical Library                           45
Washington, DC   20438


Los Alamos Scientific Laboratory
ATTN:  GMX-2, Dr. L. Smith                          46
       WX-3, Dr. A. Popolato                        47
       Technical Library                            48
Los Alamos, NM   87544


Lawrence Livermore Laboratory
ATTN:  Technical Library                            49
       Mr. B. Dobratz                               50
       Dr. F. Walker                                51
PO Box 808
Livermore, CA   94550


Sandia Corporation
ATTN:  Dr. N. Brown                                 52
       Technical Library                            53
Albuquerque, NM   87115


Air Force Office of Scientific Research            54
1400 Wilson Boulevard
Arlington, VA   22209


Stanford Research Institute
Fluid Physics & Detonation Dynamics Dept.
ATTN:  Dr. M. Cowperthwaite                         55
Menlo Park, CA   34025


U.S. Atomic Energy Commission
ATTN:  Division of Technical Information           56
Oak Ridge, TN   37830


Mr. Jack R. Polson                                 57
Mason and Hanger - Silas Mason Co.
Development Section, IAAP
Burlington, IA   52601
```

Dr. L. Yang   58
Jet Propulsion Laboratory
4800 Oak Grove Drive
Pasadena, CA 91103

Dr. Peter Mark   59
Department of Electrical Engineering
Princeton University
Princeton, NJ 08540

Dr. F. E. Williams   60
Department of Physics
University of Delaware
Newark, DE 19711

Commander
Picatinny Arsenal
ATTN: Dr. D. S. Downs, Explosives Div, FRL   61-90
Dover, NJ 07801